The signature of fluctuations of the hydrogen bond network formed by water molecules in the interfacial layer of anionic lipids

Ana-Marija Pavlek[a, 1], Barbara Pem[b, *], Danijela Bakarić[b, *]

[a] Faculty of Chemical Engineering and Technology, Trg Marka Marulića 19, 10000 Zagreb, Croatia

[b] Division of Organic Chemistry and Biochemistry, Ruđer Bošković Institute, Bijenička 54, 10000 Zagreb, Croatia

*Corresponding author. Tel.: +385 1 4571 382; E-mail: barbara.pem@irb.hr (Barbara Pem), danijela.bakaric@irb.hr (Danijela Bakarić)

Supplementary Materials

[1] Neé Ana-Marija Čižmek. Present address: Eurofins Croatiakontrola laboratory, Karlovačka 4 L, 10000 Zagreb, Croatia.

S1. Multivariate analysis of the spectral region 2980-2820 cm^{-1}

In spectral region 29820-2820 cm^{-1} (**D_1**) the bands originated from the (anti)symmetric stretching of hydrocarbon chains methylene moieties absorb ($\nu_{(a)s}CH_2$); $\nu_{as}CH_2$ at 30 °/50 °C displays maximum at 2919 cm^{-1}/2923 cm^{-1}, whereas ν_sCH_2 at 30 °/50 °C at 2850 cm^{-1}/2853 cm^{-1}, respectively [1] (Figure S1). This spectral region was baseline-corrected by a simple offset at 2820 cm^{-1} and was subjected to MCR-ALS with EFA [2] (Figure S2).

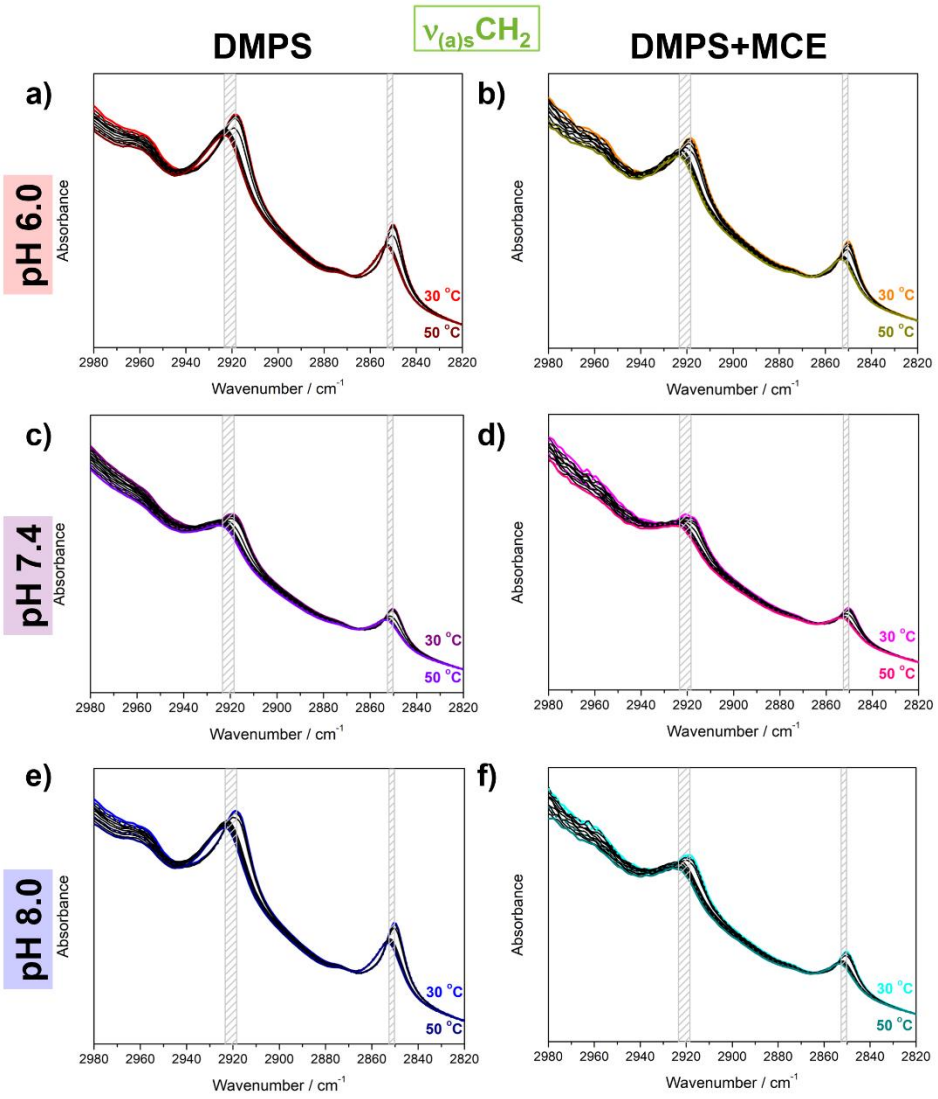

Figure S1. Baseline-corrected temperature-dependent FT-IR spectra of DMPS in the absence (left column) and the presence of MCE (right column) suspended in PBS at pH 6.0 (upper row), 7.4 (middle row), and 8.0 (bottom row). The lowest/highest (30 °C/50 °C) temperatures were highlighted with red/wine (DMPS, pH 6.0), orange/dark yellow (DMPS+MCE, pH 6.0), purple/violet (DMPS, pH 7.4), purple/pink (DMPS+MCE, pH 7.4), blue/navy (DMPS, pH 8.0) and cyan/dark cyan (DMPS+MCE, pH 8.0). The temperature-dependent FTIR spectra are designated with solid curves, whereas spectral

profiles of low- and high-temperature components obtained from MCR-ALS with EFA using dotted curves.

The concentrational profiles of low- and high-temperature components (LTC and HTC) generated by MCR-ALS in **D₁** spectral range were of sigmoid character and were fitted on a single Boltzmann profile ($R^2 \geq 0999$) (Figure S2). They resulted with the inflection points, i.e T_m values ($T_{m,1}$ for LTC and $T_{m,2}$ for HTC) [2] as follows (Figure S2, Table S1): $T_{m,\,1/2}$ = 38.5 ± 0.1 °C/38.5 ± 0.1 °C (DMPS at pH 6.0), $T_{m,\,1/2}$ = 38.2 ± 0.2 °C/38.0 ± 0.2 °C (DMPS at pH 7.4), $T_{m,\,1/2}$ = 37.7 ± 0.2 °C/37.6 ± 0.2 °C (DMPS at pH 8.0), $T_{m,\,1/2}$ = 38.3 ± 0.2 °C/38.2 ± 0.1 °C (DMPS+MCE at pH 6.0), $T_{m,\,1/2}$ = 38.0 ± 0.2 °C/37.9 ± 0.1 °C (DMPS+MCE at pH 7.4), $T_{m,\,1/2}$ = 36.9 ± 0.2 °C/37.1 ± 0.2 °C (DMPS+MCE at pH 8.0). The intersection points ($T_{m,i}$) were visually estimated to be at 38.5 °C (DMPS at pH 6.0), 38.0 °C (DMPS at pH 7.4), 37.0 °C (DMPS at pH 8.0), 38.3 °C (DMPS+MCE at pH 6.0), 37.9 °C (DMPS+MCE at pH 7.4) and 37.0 °C (DMPS+MCE at pH 8.0).

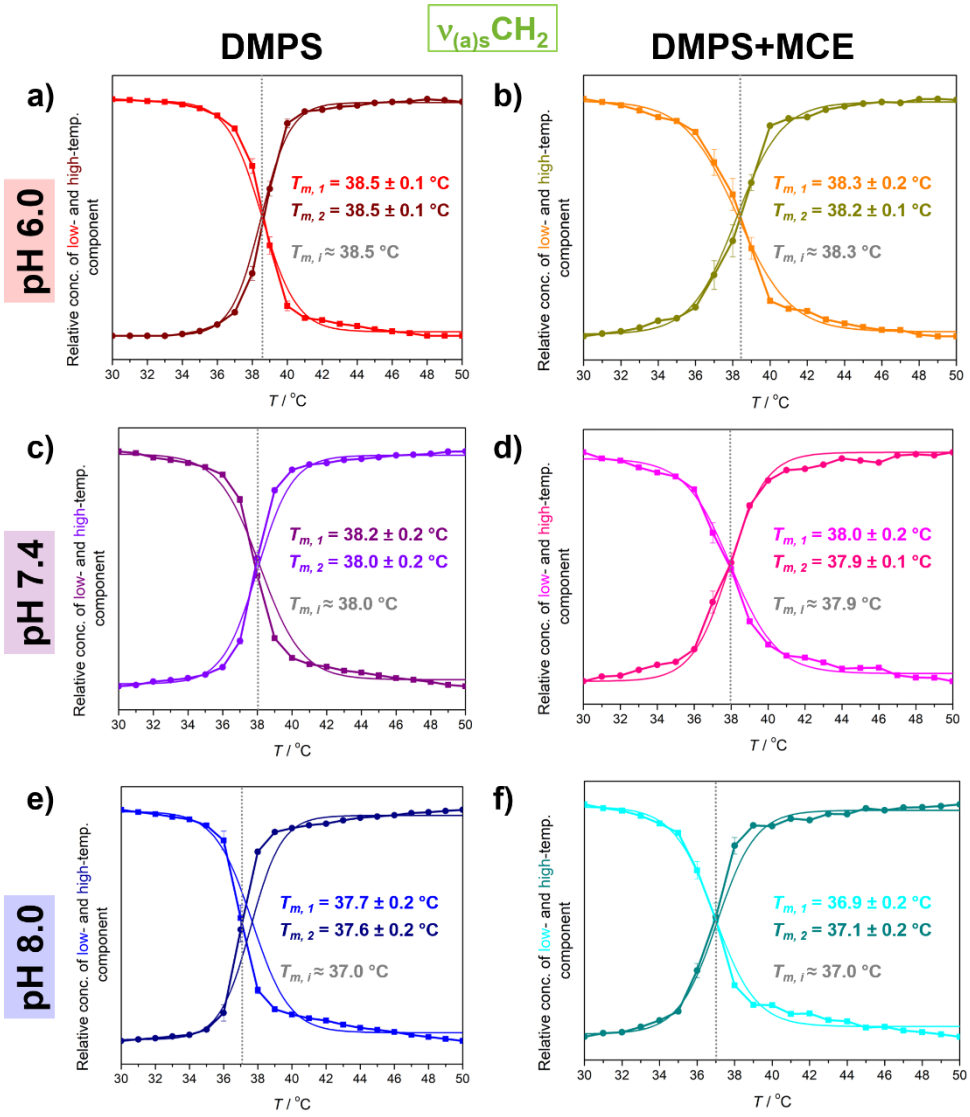

Figure S2. The concentrational profiles of low- and high-temperature component of DMPS in the absence (left column) and the presence of MCE (right column) suspended in PBS at pH 6.0 (upper row), 7.4 (middle row), and 8.0 (bottom row). Experimentally obtained low- and high-temperature components were labeled with solid curves colored red/wine (DMPS, pH 6.0), orange/dark yellow (DMPS+MCE, pH 6.0), purple/violet (DMPS, pH 7.4), purple/pink (DMPS+MCE, pH 7.4), blue/navy (DMPS, pH 8.0) and cyan/dark cyan (DMPS+MCE, pH 8.0). Their fit on a single Boltzmann profile is designated with dotted curves of the corresponding color.

Table S1. T_m values ($T_{m,1}$ and $T_{m,2}$) obtained from fitting LTC ($T_{m,1}$) and HTC ($T_{m,2}$) on a single Boltzmann profile and from the intersection point ($T_{m,i}$)

	Suspension (pH value of PBS)					
T_m[a]	DMPS			DMPS+MCE		
	6.0	7.4	8.0	6.0	7.4	8.0
$T_{m,1}$	38.5 ± 0.1	38.2 ± 0.2	37.7 ± 0.2	38.3 ± 0.2	38.0 ± 0.2	36.9 ± 0.2
$T_{m,2}$	38.5 ± 0.1	38.0 ± 0.2	37.6 ± 0.2	38.2 ± 0.1	37.9 ± 0.1	37.1 ± 0.2
$T_{m,i}$	38.5	38.0	37.0	38.3	37.9	37.0

[a] In °C.

T_m values obtained coincide with already reported [3,4] and display the change with pH value of the medium [5], especially at higher pH values. The hysteresis found between T_m values obtained from LTC ($T_{m,1}$) and HTC ($T_{m,2}$), as well as obtained from the intersection point, are in the range of uncertainty. Additionally, the sharpness of the transition is significantly reduced when MCE is incorporated in the bilayer [6].

S2. Additional molecular dynamics information

Structural parameters

Area per lipid (APL) was calculated by dividing the surface area of the *xy* plane of the simulation box by the number of lipids in one leaflet.

Membrane thickness was calculated as the distance between the average positions of phosphate atoms of opposing leaflets obtained from the number density profiles. The error was estimated from the difference between symmetrized and unsymmetrized density profiles.

The confirmation of MCE impact on membrane organization was seen from acyl chain order parameters ($-S_{CD}$), which are a measure of the degree of order of lipid acyl chains. Higher values are indicative of the gel phase, where chains are ordered, whereas in fluid phase the chains are organized more randomly and $-S_{CD}$ is low. Figure S3 shows that the addition of MCE significantly decreases the degree of order of lipid chains at both temperatures (Figure S4). The values calculated for pure DMPS bilayers are consistent with experimental determination of deuterium order parameters at 55 °C ($-S_{CD}$ ~ 0.15-0.25) [7]. Other MD simulations produced $-S_{CD}$ ~ 0.05-0.30 at 60 °C and $-S_{CD}$ ~ 0.10-0.40 at 30 °C [8], or $-S_{CD}$ ~ 0.13-0.25 at 37 °C [9], but those were conducted in the presence of 15% cholesterol or 3% amlodipine, respectively.

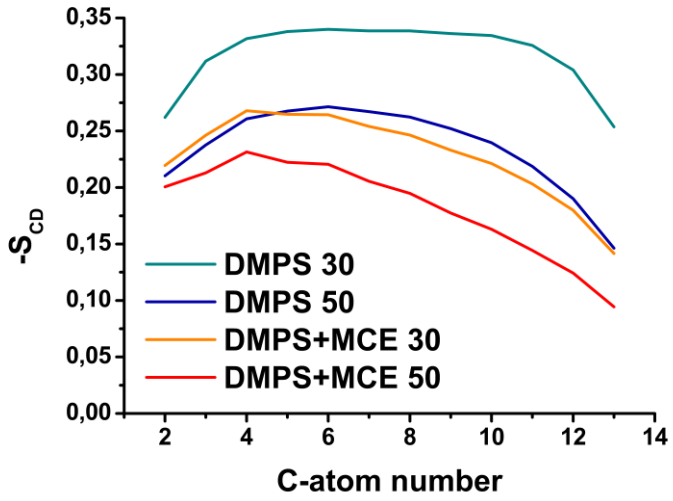

Figure S3 Order parameters of acyl chains for DMPS and DMPS+MCE systems at 30 °C and 50 °C, obtained from molecular dynamics simulations.

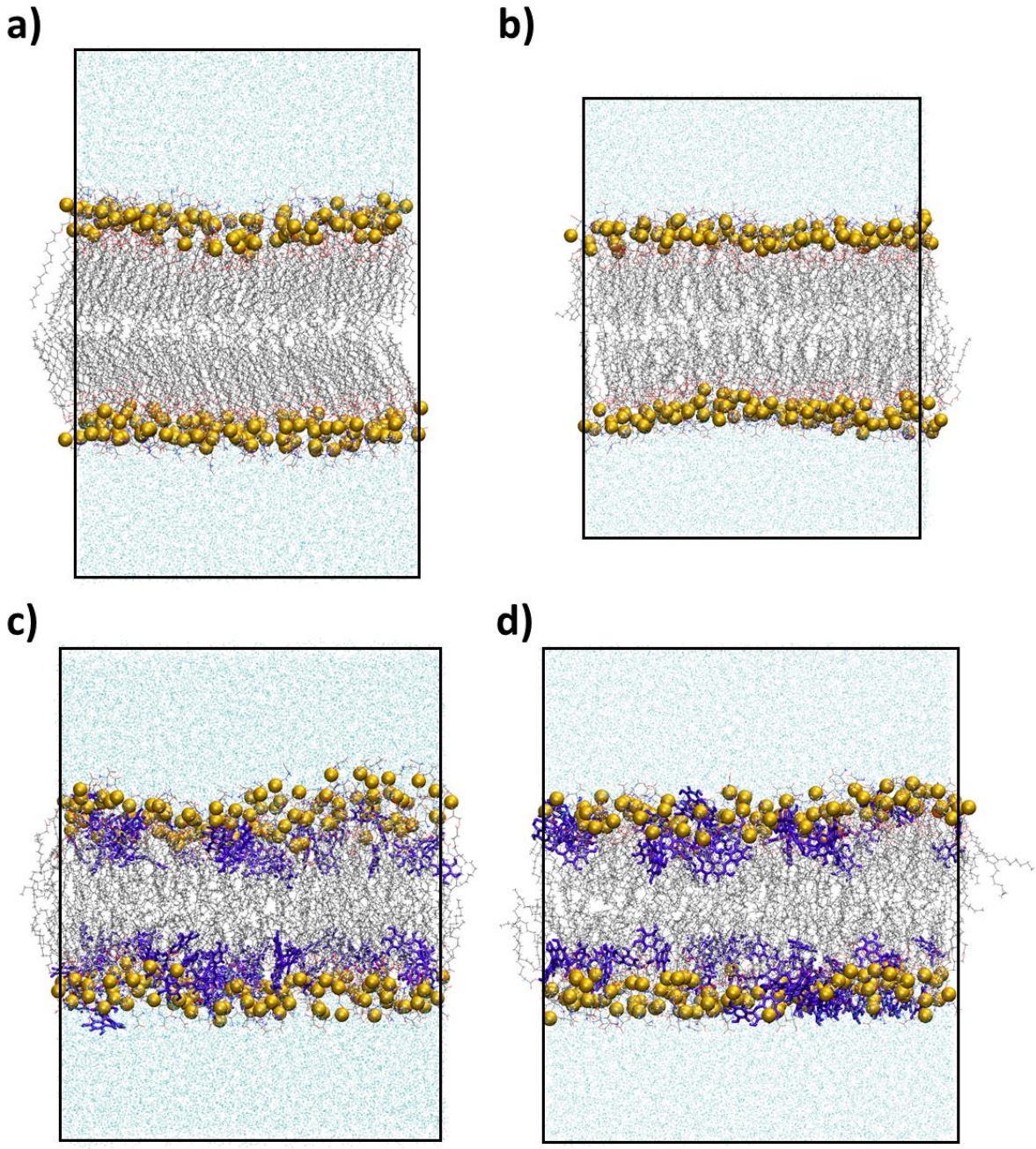

Figure S4. Representative snapshots of lipid bilayers in the production runs of molecular dynamics simulations: a) DMPS at 30 °C, b) DMPS at 50 °C, c) DMPS+MCE at 30 °C and d) DMPS+MCE at 50 °C. Lipids are shown in *Line* mode with the acyl chains painted in gray. Phosphorus atoms are shown as gold spheres. MCE is shown in *Licorice* mode in violet, and water molecules as cyan dots. Black outlines represent the edges of the simulation boxes.

Chain tilt angle is another parameter showing acyl chain ordering (Figure S5). Here, it was calculated as an angle between the vector formed by carbonyl C and terminal methyl C of each

chain with the *z* axis (membrane normal). Bilayers with a high degree of order, such as DMPS at 30 °C, have a narrow angle distribution.

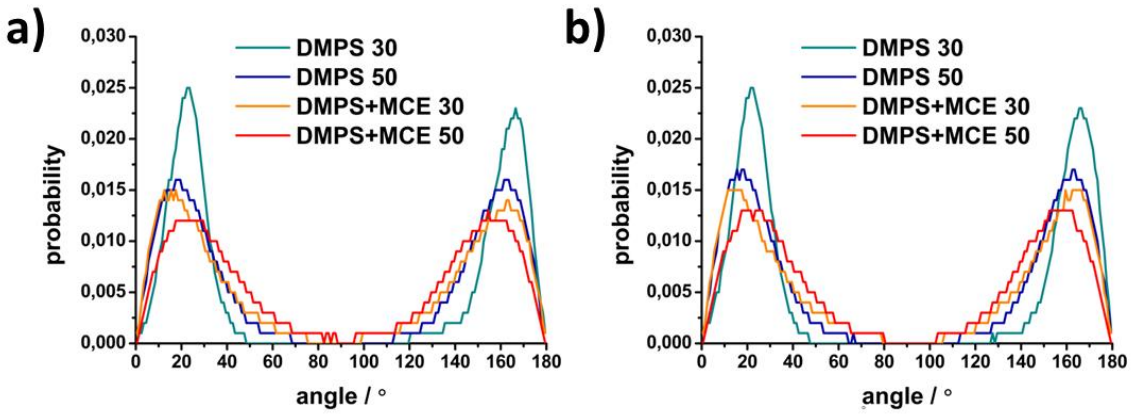

Figure S5. The histograms showing the distribution of chain tilt angles of DMPS and DMPS+MCE systems for *sn*-1 chain (a) and *sn*-2 chain (b).

Density profiles

Number density profiles show the average density of particular molecules along the *z*-axis of the simulation box. In addition to displaying water overlap with the bilayer surface, Figure 4. In the main text also shows the location of MCE inside the membrane. Though MCE is considered to be non-polar, it does contain hydroxyl groups in its structure and is thus able to form HBs with lipid headgroups and water.

Hydrogen bonds

H-bonding in MD simulations is recognized between molecules or groups when the distance between donor and acceptor is lower than 0.35 nm, and the angle H-donor-acceptor is less than 30 °. HB quantification was conducted using the gromacs *hbond* module on the 150 ns of trajectory, while the extensive network analysis was done in VMD software from 50 randomly selected frames from the last 150 ns of each simulation. Each frame, all water molecules that established a bond with DMPS were counted and selected for further analysis.

Lipid-water HB network was examined by determining the amount of “bridge” waters, i.e. water molecules that establish a HB with more than one lipid.

Table S2. The percentage of H-bonded water molecules that form a particular bonding pattern with DMPS lipids, for studied systems. Pattern 1-1 indicates one water molecule bound to one lipid. Pattern 1-2 indicates one water molecule bound to two different lipids. Pattern 1-3 indicates one water molecule bound to three lipids. Pattern 1=1 indicates one water molecule forming two bonds with the same lipid molecule. Pattern 1-12 indicates one water molecule bound to one lipid through one bond, and to one another lipid through two bonds.

Pattern	**DMPS**		**DMPS+MCE**	
	30 °C	**50 °C**	**30 °C**	**50 °C**
1-1	75.8 ± 1.9 %	80.1 ± 1.9 %	80.6 ± 2.0 %	81.7 ± 2.4 %
1-2	20.1 ± 1.2 %	16.0 ± 1.0 %	15.4 ± 0.9 %	14.2 ± 0.9 %
1-3	0.7 ± 0.2 %	0.4 ± 0.2 %	0.3 ± 0.2 %	0.4 ± 0.2 %
1=1	2.8 ± 0.4 %	3.0 ± 0.5 %	3.2 ± 0.1 %	3.3 ± 0.5 %
1-12	0.5 ± 0.2 %	0.4 ± 0.2 %	0.5 ± 0.2 %	0.4 ± 0.1 %

Water-water HB network was examined by determining additional water-water HBs that each lipid-bound water may establish with surrounding water molecules.

Table S3. The percentage of water molecules bonded to DMPS lipids, that also establish additional HBs with other waters.

Extra HBs	**DMPS**		**DMPS+MCE**	
	30 °C	**50 °C**	**30 °C**	**50 °C**
0	28.1 ± 1.5 %	25.9 ± 1.4 %	23.9 ± 1.1 %	24.7 ± 1.1 %
1	39.5 ± 1.7 %	40.2 ± 1.7 %	39.3 ± 1.5 %	40.2 ± 1.6 %
2	25.0 ± 1.2 %	26.1 ± 1.2 %	27.7 ± 1.5 %	26.9 ± 1.3 %
3	7.4 ± 0.7 %	7.8 ± 0.8 %	9.1 ± 0.8 %	8.2 ± 0.9 %

Water molecules that established at least one HB with lipids, were examined further for bonding with other waters. Each water molecule could establish between 0 and 3 additional HBs with interfacial water.

Literature:

1. Lewis, R.N.A.H.; McElhaney, R.N. Membrane Lipid Phase Transitions and Phase Organization Studied by Fourier Transform Infrared Spectroscopy. *Biochim. Biophys. Acta - Biomembr.* **2013**, *1828*, 2347–2358, doi:10.1016/j.bbamem.2012.10.018.

2. Maleš, P.; Brkljača, Z.; Crnolatac, I.; Bakarić, D. Application of MCR-ALS with EFA on FT-IR Spectra of Lipid Bilayers in the Assessment of Phase Transition Temperatures: Potential for Discernment of Coupled Events. *Colloids Surfaces B Biointerfaces* **2021**, *201*, 111645, 8, doi:10.1016/j.colsurfb.2021.111645.

3. Bach, D.; Miller, I.R. Hydration of Phospholipid Bilayers in the Presence and Absence of Cholesterol. *Biochim. Biophys. Acta* **1998**, *1368*, 216–224, doi:10.1016/j.chemphyslip.2005.04.001.

4. Schönfeldová, T.; Piller, P.; Kovacik, F.; Pabst, G.; Okur, H.I.; Roke, S. Lipid Melting Transitions Involve Structural Redistribution of Interfacial Water. *J. Phys. Chem. B* **2021**, *125*, 12457–12465, doi:10.1021/acs.jpcb.1c06868.

5. Heimburg, T. *Thermal Biophysics of Membranes*; Wiley-VCH Verlag GmbH, Ed.; Weinheim, 2007; ISBN 9783527404711.

6. Šegota, S.; Vojta, D.; Kendziora, D.; Ahmed, I.; Fruk, L.; Baranović, G. Ligand-Dependent Nanoparticle Clustering within Lipid Membranes Induced by Surrounding Medium. *J. Phys. Chem. B* **2015**, *119*, 5208–5219, doi:10.1021/acs.jpcb.5b00898.

7. Browning, J.L.; Seelig, J. Bilayers of Phosphatidylserine: A Deuterium and Phosphorus Nuclear Magnetic Resonance Study. *Biochemistry* **1980**, *19*, 1262–1270, doi:10.1021/bi00547a034.

8. Boughter, C.T.; Monje-Galvan, V.; Im, W.; Klauda, J.B. Influence of Cholesterol on Phospholipid Bilayer Structure and Dynamics. *J. Phys. Chem. B* **2016**, *120*, 11761–11772, doi:10.1021/acs.jpcb.6b08574.

9. Yousefpour, A.; Amjad-Iranagh, S.; Goharpey, F.; Modarress, H. Effect of Drug Amlodipine on the Charged Lipid Bilayer Cell Membranes DMPS and DMPS + DMPC: A Molecular Dynamics Simulation Study. *Eur. Biophys. J.* **2018**, *47*, 939–950, doi:10.1007/s00249-018-1317-z.